

# Correcting soil water balance calculations for dew, fog, and light rainfall

R. Moratiel · D. Spano · P. Nicolosi ·  
R. L. Snyder

Received: 31 August 2011 / Accepted: 15 December 2011 / Published online: 10 January 2012  
© Springer-Verlag 2012

**Abstract** In Mediterranean climates, adoption and use of the ET-based scheduling method is limited to regions characterized by considerable contributions to evapotranspiration from fog interception, dew, and light rainfall. While the crop evapotranspiration is often accurately estimated, the water balance is frequently in error because a considerable portion of the energy expended is used to vaporize water from the plant surfaces rather than from inside the leaves (i.e., transpiration). Growers in regions with considerable fog, dew, and light rainfall are hesitant to use ET-based scheduling because the cumulative crop evapotranspiration between irrigations is often considerably higher than the soil water depletion. A correction for these surface contributions is clearly needed to improve the water balance calculations and to enhance adoption of the

ET-based scheduling method. In this paper, we present a simple, practical method to estimate the contribution of fog interception, dew, and light rainfall to daily crop evapotranspiration, and we show how to use the method to improve water balance calculations.

## Introduction

Surface vaporization and soil water depletion

The main sources of water for an irrigated crop include irrigation applications, precipitation, water table, fog interception, and dew formation. For a well-drained soil in a climate where there are few events of fog, dew, or light rainfall, computing a water balance is relatively easy. However, it is hard to determine a water balance in locations with considerable fog, dew, or light rainfall. In regions with high evaporative demand, the contributions of these sources are relatively small and difficult to quantify, but when the crop evapotranspiration ( $ET_c$ ) rates are also small, the fog, dew, and light rainfall contributions are important. In water balance irrigation scheduling, the goal is to estimate soil water depletions using evapotranspiration. However, soil water depletion ( $D_S$ ) is over-estimated if a considerable portion of the water supply comes from surface vaporization ( $V_S$ ) rather than from  $D_S$ . Thus, it is important to differentiate the source of water contributing to evapotranspiration in order to use water efficiently. When plant foliage is wet, regardless of the weather conditions, surface evaporation reduces transpiration losses because energy that would contribute to transpiration is consumed in the evaporation process on the leaf surfaces. The main impact of  $V_S$  from a wet crop surface is to reduce the contribution of soil water to  $ET_c$ . Correcting for  $V_S$

---

Communicated by A. Kassam.

R. Moratiel (✉)  
Department of Plant Production, Universidad Politécnica  
de Madrid, Avda. Complutense s/n, 28040 Madrid, Spain  
e-mail: ruben.moratiel@upm.es

R. Moratiel  
CEIGRAM, Centro de Estudios e Investigación para la Gestión  
de Riesgos Agrarios y Medioambientales, C/Senda del Rey 13,  
28040 Madrid, Spain

D. Spano  
Department of Economics and Woody Plants (DESA),  
University of Sassari, 07100 Sassari, Italy

P. Nicolosi  
Department Di Colture Arbore, University of Palermo, Palermo,  
Italy

R. L. Snyder  
Department of Land, Air and Water Resources,  
University of California Davis, Davis, CA 95616, USA

contributions is therefore an important factor for efforts to use irrigation water efficiently in environments with dew, fog, and light rainfall.

Fog forms when there are condensation particles in the air, the air temperature falls to near the dew point temperature, and there is a light to moderate breeze. When fog moves in the air and strikes plant canopies, some of the fog is intercepted and coats plant parts with water and wets the soil surface. In some regions, fog coating of plants and fog drip can provide an important fraction of the annual water balance (Dawson 1998). In general, fog formation occurs at night when the minimum daily temperature is lower than the mean daily dew point temperature. Figure 1 is a plot of the difference between the July mean daily minimum and dew point temperatures versus the mean daily minimum temperature for 129 California Irrigation Management Information System (CIMIS) weather stations (Snyder and Pruitt 1992). The plot illustrates that 36 sites have daily minimum temperatures consistently below the mean daily dew point temperature even in July. Most of the 36 sites are in locations having lower minimum temperatures. This implies that vegetation in those locations is likely to experience fog interception. Reference evapotranspiration ( $ET_o$ ) is a measure of the evaporative demand of the atmosphere (Doorenbos and Pruitt 1977), having canopy resistance  $r_c = 70 \text{ s m}^{-1}$  and aerodynamic resistance  $r_a = 208/U_2 \text{ s m}^{-1}$ , where  $U_2$  is the wind speed in  $\text{m s}^{-1}$  measured at 2-m height over grass (Allen et al. 2005). Actually,  $ET_o$  is approximately equal to the evapotranspiration of a broad expanse of 0.12-m-tall grass. The midsummer  $ET_o$  at stations with daily dew point temperatures less than the minimum daily temperature varies from 3 to  $4 \text{ mm day}^{-1}$ . The authors have observed 1–2 mm day of fog interception dripping into rain gauges in some of these regions during July when the daily  $ET_o$  rate was on the order of 2–3  $\text{mm day}^{-1}$ . In the winter, when daily  $ET_o$  rates are on

the order of 1–2  $\text{mm day}^{-1}$ , the authors have actually observed weight gain on precision lysimeters on foggy winter days. Clearly, fog interception can be an important source of water for evapotranspiration. Note that fog interception has little direct effect on  $ET_c$  except that wet plants will have canopy resistance equal to zero. Therefore, when plants are wet, a small error in the  $ET_o$  and  $ET_c$  estimation is expected because the standardized  $ET_o$  equation has a nonzero canopy resistance. Evaporation of intercepted fog water requires energy, however, and this can greatly reduce the energy used for transpiration of soil moisture from a crop. Therefore, the main effect of fog interception is to reduce water extraction from of soil water.

Dew forms when the surface temperature is lower than or equal to the dew point temperature, and the water vapor from the air in contact with the cold surface condenses to form dew. Like fog, dew is most likely to form when the daily minimum temperature is less than the mean daily dew point temperature; however, it is more likely to form under calm wind conditions or in the absence of condensation particles in the air. Dew depends particularly on local nocturnal microclimate and thus varies to a great extent even within the same area (Moro et al. 2007). Most research on dew was conducted in natural rather than crop ecosystems (Katoka et al. 2010; Kidron 1999; Mildenerger et al. 2009; Moro et al. 2007; Prada et al. 2009). Jacobs et al. (2006) reported that 4.5% of the precipitation onto grassland in the Netherlands came from dew, and many coastal locations, such as in California, have good conditions for dew deposition even in July (Fig. 1). Clearly, ignoring dew contributions to the water balance can lead to errors in some locations.

While the initial abstraction of light rainfall, which coats the crop surfaces, is often ignored as a source of water for evapotranspiration, it can be important in areas where frequent light rainfall is common and evapotranspiration rates are low. In light rainfall areas, tipping bucket rain gauges often under estimate the true rainfall because insufficient quantities of water fall into the bucket to cause tipping. Since the depth of light rainfall is spatially variable and difficult to measure, and most or all light rainfall will contribute to  $V_S$  and reduce the energy used for transpiration, that is, soil water depletion, some method other than rainfall depth is needed to correctly account for the light rainfall. Again, this can lead to under estimation of the rainfall contribution to evapotranspiration and proper accounting can improve irrigation scheduling and the efficient use of water.

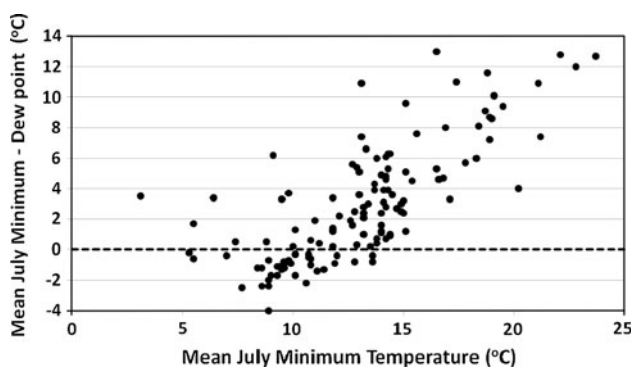


**Fig. 1** A plot of the differences between the July mean daily minimum and dew point temperatures ( $^{\circ}\text{C}$ ) versus the mean July minimum temperature ( $^{\circ}\text{C}$ ) for 129 CIMIS stations in California. Thirty-six stations had negative differences between the daily minimum and dew point temperatures

## Irrigation management

Good irrigation scheduling requires information on the soil water depletion within the crop root zone, application

uniformity and efficiency, and the application rate ( $A_R$ ). The soil water depletion ( $D_S$ ) is the difference between the volumetric water content at field capacity and the soil volumetric water content, where field capacity is the soil water content reached after drainage of the gravitational water. Ignoring leaching fractions for salinity management, the net irrigation application needed to refill the soil to field capacity is equal to the  $D_S$  before irrigation. The distribution uniformity ( $D_U$ ) is a measure of how evenly water soaks in across the field, and the application efficiency is an estimate of the fraction of water applied that wets the crop and soil and is stored in the soil where it can contribute to evapotranspiration. For good irrigation management, when adequate irrigation water is available, the irrigator should optimize the  $D_U$  and application efficiency ( $A_E$ ). It is therefore important to distribute the water uniformly to the crop and to apply the correct depth of water to minimize deep percolation and runoff and to supply sufficient water such that most of soil reservoir is refilled to field capacity. If the net application ( $A_N$ ) is set equal to  $D_S$ , then dividing  $A_N$  by the  $D_U$  gives an estimate of the required gross application ( $A_G$ ) or “applied water” to force  $D_U \approx A_E$ . This will refill most of the soil to field capacity. The system set time is calculated as  $A_G/A_R$ . Identifying accurate estimates of  $D_S$  before irrigation is an important component of the scheduling process (Letey et al. 2007), so correcting the water balance calculation for  $V_S$  is needed for accurate irrigation where plant surface water is considerable.

The two main methods to determine  $D_S$  are to measure soil moisture or, for well-drained soils, to measure cumulative crop evapotranspiration ( $CET_c$ ). Water balance scheduling is usually based on the idea that cumulative  $ET_c$  on each day provides an estimate of the change in soil moisture on each day. Therefore, if there are no unknown sources of water (e.g., fog, dew, light rainfall, or water tables), the  $CET_c$  after wetting the soil to field capacity provides an estimate of the  $D_S$ . For a well-managed irrigated crop, most of the water loss is due to  $ET_c$ . Other possible losses include deep percolation and runoff, which are accounted for by the irrigation application efficiency, where the application efficiency is roughly equal to the applied water that evaporates divided by the total applied water.

There is a transition from  $V_S$  to  $D_S$  contributions to  $ET_c$  as the surface water dries from a crop. One method to estimate the daily  $V_S$  contribution is to calculate the  $ET_c$  up to the time when the plant dries. The questions are as follows: (1) how does one calculate the  $V_S$  contribution? and (2) is the method spatially and temporally accurate? Once the  $V_S$  is known, the daily soil water depletion ( $D_S$ ) equals the daily  $ET_c$  minus the  $V_S$  contribution. To our knowledge, there is no evapotranspiration-based method available to estimate  $D_S$  that accounts for  $V_S$ . The aim of this study was to develop a simple, practical procedure to

estimate the contribution of fog interception, dew, and light rainfall to daily crop evapotranspiration and to show how to use the information to improve water balance calculations for efficient water use in irrigation.

## Methods

It is assumed that the relationship between normalized hourly  $ET_o$  and time of the day is similar to the relationship between normalized hourly  $ET_c$  and time of the day. Therefore, the analysis to find a model for normalized  $ET_o$  as a function of time was developed, and it is assumed that the same relationship will apply to a well-watered crop  $ET_c$ .

Hourly climate data from 2007 were collected from 30 California Irrigation Management Information System (CIMIS) weather stations (Snyder and Pruitt 1992). The station details are described in Table 1, and the general locations are shown in Fig. 2. Hourly standardized reference evapotranspiration for short canopies was calculated following the procedures in Allen et al. (2005) using Eq. 1 and hourly climate data, which included solar radiation ( $W\ m^{-2}$ ), air temperature ( $^{\circ}C$ ), dew point temperature ( $^{\circ}C$ ), and wind speed at 2 m height ( $m\ s^{-1}$ ). The data were hourly means of 1-min samples.

$$ET_{oi} = \frac{0.408\Delta(R_n - G) + \gamma \frac{37}{T+273} u_2 (e_a - e_d)}{\Delta + \gamma(1 + 0.34u_2)} \quad (1)$$

where  $ET_{oi}$  ( $mm\ h^{-1}$ ) is reference evapotranspiration for the  $i$  th hour of the day,  $R_n$  ( $MJ\ m^{-2}\ h^{-1}$ ) is net radiation over a well-watered grass,  $G$  ( $MJ\ m^{-2}\ h^{-1}$ ) is soil heat flux density,  $T$  ( $^{\circ}C$ ) is mean hourly temperature,  $\Delta$  ( $kPa\ ^{\circ}C^{-1}$ ) is the slope of the saturation vapor pressure curve at  $T$ ,  $\gamma$  ( $kPa\ ^{\circ}C^{-1}$ ) psychrometric constant,  $e_a$  ( $kPa$ ) is the saturation vapor pressure at temperature  $T$ ,  $e_d$  ( $kPa$ ) is the saturation vapor pressure at the dew point temperature or the hourly actual vapor pressure, and  $u_2$  ( $m\ s^{-1}$ ) is the mean hourly wind speed.

The daily total  $ET_{od}$  ( $mm\ day^{-1}$ ) was calculated from the  $ET_{oi}$  values as:

$$ET_{od} = \sum_{i=1}^{24} ET_{oi} \quad (2)$$

for hours  $i = 1-24$  for each day and station. The normalized cumulative evapotranspiration ( $NET_{oh}$ ) was computed for each CIMIS station for each hour of each day using the equation:

$$NET_{oh} = \frac{\sum_{i=1}^h ET_{oi}}{ET_{od}} \quad (3)$$

for hours  $h = 1-24$ . The monthly means of the hourly  $NET_{oh}$  were determined for each station to investigate

**Table 1** CIMIS station names, numbers, latitude, longitude, elevation, and annual reference evapotranspiration ( $ET_0$ ) that were used in the analysis

| CIMIS station name | Number | Latitude (°) | Longitude (°) | Elevation (m) | Annual 2007 $ET_0$ (mm) |
|--------------------|--------|--------------|---------------|---------------|-------------------------|
| Barstow NE         | 134    | 34.9         | 117.0         | 621.8         | 1,849                   |
| Bishop             | 35     | 37.4         | 118.4         | 1,271.0       | 1,531                   |
| Blythe NE          | 135    | 33.6         | 114.7         | 83.8          | 2,006                   |
| Camino             | 13     | 38.8         | 120.7         | 847.3         | 1,446                   |
| Castroville        | 19     | 36.8         | 121.8         | 2.7           | 810                     |
| Davis              | 6      | 38.3         | 121.5         | 18.3          | 1,464                   |
| Escondido SPV      | 153    | 33.1         | 117.0         | 118.9         | 1,422                   |
| Fresno State       | 80     | 36.8         | 119.7         | 103.3         | 1,447                   |
| Gerber             | 8      | 40.1         | 122.2         | 76.2          | 1,467                   |
| Indio 2            | 200    | 33.8         | 116.3         | 12.2          | 1,975                   |
| Irvine             | 75     | 33.7         | 117.7         | 125.0         | 1,332                   |
| King City Oasis Rd | 113    | 36.1         | 121.1         | 164.6         | 1,324                   |
| Manteca            | 70     | 37.8         | 121.2         | 21.3          | 1,423                   |
| Nipomo             | 202    | 35.0         | 120.6         | 77.7          | 994                     |
| Orland             | 61     | 39.7         | 122.2         | 60.4          | 1,447                   |
| Oxnard             | 156    | 34.2         | 119.2         | 14.6          | 1,084                   |
| Parlier            | 39     | 36.6         | 119.5         | 102.7         | 1,642                   |
| Petaluma East      | 144    | 38.3         | 122.6         | 29.6          | 1,054                   |
| Salinas South      | 89     | 36.6         | 121.5         | 36.6          | 1,143                   |
| San Diego II       | 184    | 32.7         | 117.1         | 115.0         | 1,184                   |
| Sanel Valley       | 106    | 39.0         | 123.1         | 160.0         | 1,282                   |
| Santa Monica       | 99     | 34.0         | 118.5         | 103.6         | 1,183                   |
| Santa Ynez         | 64     | 34.6         | 120.1         | 149.4         | 1,276                   |
| Shafter            | 5      | 35.5         | 119.3         | 33.5          | 1,464                   |
| Torrey Pines       | 173    | 32.9         | 117.3         | 102.1         | 992                     |
| Tulelake           | 91     | 42.0         | 121.5         | 1,229.9       | 1,231                   |
| Twitchell Island   | 140    | 38.1         | 121.7         | -0.3          | 1,478                   |
| Union City         | 171    | 37.6         | 122.1         | 4.9           | 1,028                   |
| West Side Fld Sta  | 2      | 36.3         | 120.1         | 86.9          | 1,642                   |
| Winchester         | 179    | 33.7         | 117.1         | 495.6         | 1,469                   |



**Fig. 2** Location of the 30 CIMIS weather stations in California used in this study

spatial and seasonal variation. Then, the monthly means and standard deviations over stations were calculated to determine a general model for  $V_S$  and  $D_S$  contributions to evapotranspiration.

## Results and discussion

Climate data for three representative CIMIS stations are listed in Table 2. One concern with this approach to

**Table 2** Climate data including solar radiation ( $R_s$ ), maximum temperature ( $T_x$ ), minimum temperature ( $T_n$ ), wind speed at 2 m height ( $U_2$ ), dew point temperature ( $T_d$ ), precipitation ( $P_{cp}$ ), and reference evapotranspiration ( $ET_o$ ) for Davis, Indio<sup>a</sup>, and Torrey Pines CIMIS stations

| Station      | Mon | $R_s$<br>(MJ m <sup>-2</sup> day <sup>-1</sup> ) | $T_x$<br>(°C) | $T_n$<br>(°C) | $U_2$<br>(m s <sup>-1</sup> ) | $T_d$<br>(°C) | $P_{cp}$<br>(mm) | $ET_o$<br>(mm day <sup>-1</sup> ) |
|--------------|-----|--|---------------|---------------|-------------------------------|---------------|------------------|-----------------------------------|
| Davis        | 1   | 2.7  | 5.1           | 1.2           | 1.0                           | 1.9           | 71.8             | 1.0                               |
|              | 2   | 10.4   | 21.7          | 4.3           | 2.7                           | 5.7           | 91.6             | 1.7                               |
|              | 3   | 15.3   | 18.9          | 5.9           | 2.7                           | 6.8           | 104.0            | 3.0                               |
|              | 4   | 21.0   | 22.1          | 7.0           | 2.9                           | 6.4           | 19.5             | 4.6                               |
|              | 5   | 25.0   | 26.3          | 9.9           | 3.0                           | 8.2           | 14.9             | 5.9                               |
|              | 6   | 28.2   | 30.1          | 12.4          | 3.0                           | 10.3          | 8.8              | 7.1                               |
|              | 7   | 28.8   | 32.9          | 13.3          | 2.7                           | 12.1          | 5.6              | 7.0                               |
|              | 8   | 26.7   | 32.8          | 13.0          | 2.5                           | 12.0          | 5.5              | 6.2                               |
|              | 9   | 22.1   | 31.4          | 12.4          | 2.5                           | 10.0          | 12.4             | 5.0                               |
|              | 10  | 16.5   | 27.7          | 10.4          | 2.4                           | 7.6           | 12.8             | 3.5                               |
|              | 11  | 10.3   | 20.4          | 6.7           | 2.4                           | 6.1           | 60.3             | 1.7                               |
|              | 12  | 6.9  | 13.9          | 3.2           | 2.6                           | 4.5           | 81.1             | 1.0                               |
| Indio        | 1   | 11.6   | 21.4          | 6.7           | 2.2                           | 1.0           | 14.2             | 2.5                               |
|              | 2   | 14.3   | 21.3          | 8.0           | 2.5                           | 1.8           | 16.8             | 3.1                               |
|              | 3   | 19.9   | 25.6          | 11.7          | 3.1                           | 3.1           | 10.9             | 5.3                               |
|              | 4   | 24.8   | 28.3          | 14.8          | 3.8                           | 3.2           | 1.3              | 7.1                               |
|              | 5   | 27.7   | 33.3          | 19.4          | 4.1                           | 5.9           | 1.8              | 8.6                               |
|              | 6   | 28.7   | 37.2          | 22.9          | 4.1                           | 8.6           | 0.3              | 9.3                               |
|              | 7   | 27.1   | 40.5          | 26.0          | 3.6                           | 10.0          | 1.0              | 8.8                               |
|              | 8   | 25.0   | 39.8          | 26.0          | 3.1                           | 13.0          | 13.7             | 8.0                               |
|              | 9   | 22.4   | 38.2          | 24.0          | 3.2                           | 9.8           | 1.0              | 7.1                               |
|              | 10  | 18.3   | 33.5          | 19.0          | 2.9                           | 7.2           | 6.6              | 4.8                               |
|              | 11  | 13.6   | 26.1          | 12.7          | 2.6                           | 4.4           | 4.6              | 3.1                               |
|              | 12  | 11.2   | 21.5          | 6.6           | 2.2                           | 0.5           | 15.7             | 2.2                               |
| Torrey Pines | 1   | 11.1   | 16.9          | 9.0           | 1.8                           | 6.2           | 23.1             | 1.8                               |
|              | 2   | 13.1   | 16.5          | 9.2           | 1.9                           | 7.4           | 52.2             | 2.1                               |
|              | 3   | 16.2   | 16.1          | 9.2           | 1.9                           | 8.1           | 26.8             | 2.7                               |
|              | 4   | 20.6   | 15.6          | 9.3           | 1.9                           | 8.6           | 13.8             | 3.3                               |
|              | 5   | 20.2   | 16.4          | 11.2          | 1.8                           | 10.6          | 7.6              | 3.1                               |
|              | 6   | 20.0   | 18.1          | 13.9          | 1.8                           | 12.8          | 0.0              | 3.5                               |
|              | 7   | 22.0   | 20.4          | 16.0          | 1.7                           | 15.6          | 0.0              | 3.8                               |
|              | 8   | 20.8   | 21.2          | 16.7          | 1.6                           | 16.0          | 0.6              | 3.8                               |
|              | 9   | 19.4   | 21.3          | 16.1          | 1.5                           | 15.4          | 6.7              | 3.1                               |
|              | 10  | 14.6   | 19.8          | 14.5          | 1.6                           | 13.5          | 10.5             | 2.3                               |
|              | 11  | 11.6   | 19.5          | 13.1          | 1.5                           | 11.0          | 11.3             | 1.9                               |
|              | 12  | 10.1   | 17.6          | 9.5           | 1.8                           | 7.0           | 21.9             | 1.6                               |

<sup>a</sup> Precipitation data are not collected at the Indio CIMIS station. The presented precipitation data are from a nearby National Climatic Data Center station

estimating  $V_S$  contributions is that there might be excessive variability in the  $NET_{oh}$  versus time depending on the month. Plots of the normalized  $NET_{oh}$  versus local standard time for stations in distinctly different climates are shown for Davis (Fig. 3), Indio (Fig. 4), and Torrey Pines (Fig. 5). The curve obtained was sigmoidal regardless of the season or location. Only the results for March, June, September, and December are shown, but the other months generally fell within the same range for  $NET_{oh}$ . The same curves for the other 27 stations showed the same general pattern for  $NET_{oh}$  versus the local standard time. For any

given hour, the range of the  $NET_{oh}$  was always within about 5% of the daily total.

Because the patterns of  $NET_{oh}$  versus local standard time were similar for all stations, the mean and standard deviation of the hourly cumulative  $ET_o$  by month was calculated over the 30 stations. A plot of the mean, with standard deviation bars, of the  $NET_{oh}$  versus the local standard time hour is shown in Fig. 6. The equation:

$$NET_{oh} = 1 - \frac{1}{1 + e^{\left(\frac{h-h_0}{\Delta h}\right)}} \tag{4}$$

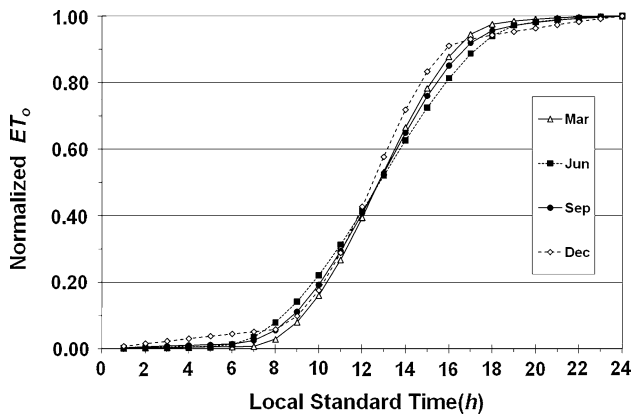


**Fig. 3** Plot of the mean normalized hourly  $NET_{oh}$  versus hour of the day local standard time ( $h$ ) for March, June, September, and December 2007 from Davis, California

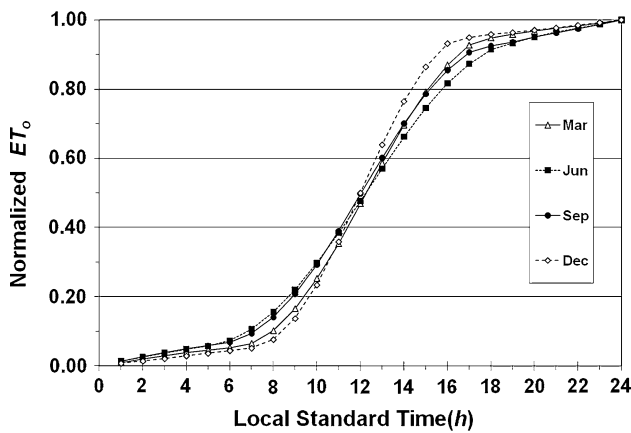


**Fig. 4** Plot of the mean normalized hourly  $NET_{oh}$  versus hour of the day local standard time ( $h$ ) for March, June, September, and December 2007 from Indio, California

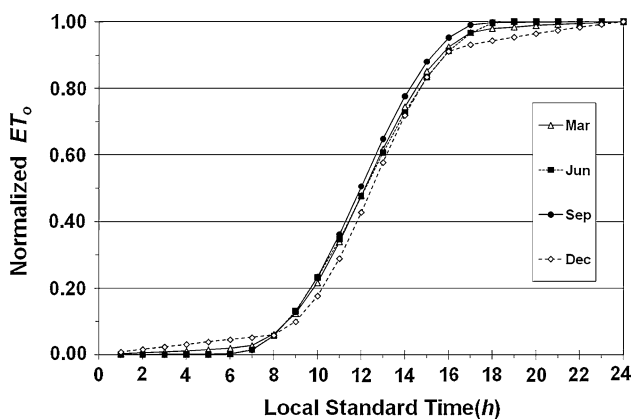


**Fig. 5** Plot of the mean normalized hourly  $NET_{oh}$  versus hour of the day local standard time ( $h$ ) for March, June, September, and December 2007 from Torrey Pines near La Jolla, California

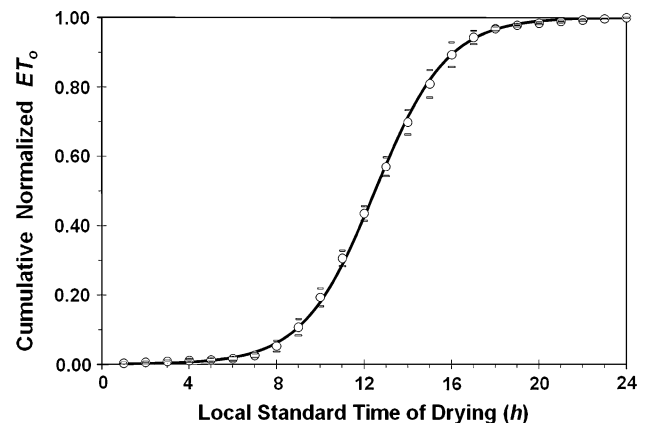


**Fig. 6** Plot of the cumulative normalized hourly  $NET_{oh}$  versus hour of the day local standard time ( $h$ ) averaged over the 12 months and over the 30 stations versus local standard time. Error bars indicate one standard deviation of the cumulative normalized  $NET_{oh}$

where  $h$  is the local standard time (hour of the day),  $h_o = 12.5$  was the time when  $NET_{oh} = 0.5$ , and  $d_h = 1.7$  was the best fit x-increment giving a RMSE = 0.032 for the predicted versus observed  $NET_{oh}$  values. The best fit for the x-increment was determined using Eq. 4, and the solver function in MS Excel to vary the values for  $d_h$  until the minimum value RMSE = 0.032 between the predicted and observed  $NET_{oh}$  was found. Therefore, Eq. 4 provides a good approximation for the  $NET_{oh}$  as a function of the local standard time for a wide range of locations with greatly different climates. If the plants are wet from fog, dew, or light rainfall, and they are observed to dry off at a particular time during the day, one can estimate the  $V_S$  using Fig. 6 or by inserting the local standard time into Eq. 4. The actual amount of water evaporated from the surface is determined by multiplying the estimate of  $NET_{oh}$  by the observed  $ET_o$  on the day of interest.

The largest uncertainty in using this method is likely due to the estimation of the time  $h$  when the plant surface dries, so it is assumed that this normalized method will apply equally well to crop evapotranspiration ( $ET_c$ ) as to  $ET_o$ . Since the total  $ET_c$  for a day is partitioned into the  $V_S$  contribution and the  $D_S$  contribution, the fraction of  $ET_c$  coming from the soil ( $F$ ), that is, the  $D_S$  contribution, would be calculated as:

$$F = \frac{1}{1 + e^{\left(\frac{t-12.5}{1.7}\right)}} \quad (5)$$

where  $t$  is the local standard time in hours. A plot of the relationship is shown in Fig. 7. The selection of the time of drying is subjective, but generally there is a fairly rapid change in canopy wetness once some of the leaf surface starts to dry. Usually, going from wet to mostly dry occurs over about an hour period, so selecting the midpoint of the hour should provide a fairly accurate estimate for

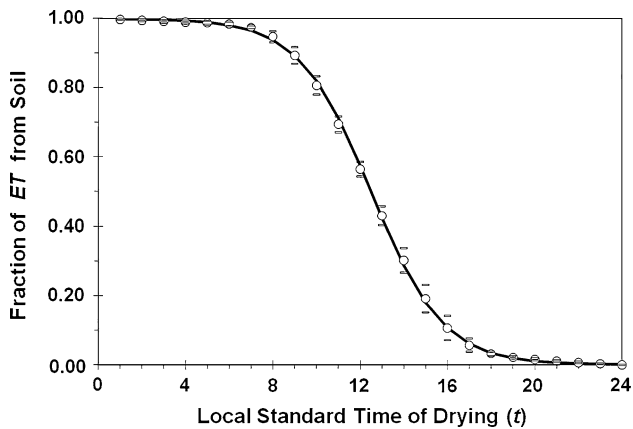


**Fig. 7** Plot of the fraction ( $F$ ) of  $ET$  coming from stored soil water as a function of hour of the day local standard time ( $t$ ) when water approximately dries from the canopy. Hourly averages are over the 12 months and over the 30 stations versus local standard time. *Error bars* indicate one standard deviation of the fraction of  $ET$  from the soil

determining  $F$ . For example, suppose that the  $ET_c$  is 4.5 mm on a day when a canopy mostly dries off between 10:00 and 11:00 a.m. local standard time. Using Fig. 7 and  $t = 10:30$  a.m., the value  $F = 0.75$  is estimated for the fraction of  $ET_c$  coming from the soil. Alternatively, using Eq. 3, the value is  $F = 0.76$ . Then, the change in soil water depletion ( $\Delta D_{SW}$ ) on that day is estimated as:

$$\Delta D_{SW} = ET_c \times F = 4.5 \times 0.76 = 3.4 \text{ mm.} \quad (6)$$

Using this correction greatly improves the estimation of soil water depletion and can boost the adoption of ET-based irrigation scheduling in regions where fog, dew, and light rainfall are common.

The technique presented in this paper provides a practical method for the estimation of dew, fog, and light rainfall contributions to crop water balance. The use of leaf wetness sensors or Penman–Monteith equation estimates of leaf wetness (Sentelhas et al. 2006) could also provide a method to make visual estimation of the time of drying less dependent on observation. The use of higher order models (e.g., Kataka et al. 2010) could improve regional estimates of  $V_S$  contributions to the water balance as well. However, the immediate benefits from using the observed time of drying to account for dew, fog, and light rainfall contribution to the water balance are considerable and are needed now.

## Conclusions

The use of ET-based irrigation scheduling has seen little adoption in regions where contributions of fog, dew, and

light rainfall to well-watered crop evapotranspiration ( $ET_c$ ) are considerable. In this paper, a relatively simple, practical method to estimate the fraction of  $ET_c$  coming from the soil was presented in graphical (Fig. 7) and equation (Eq. 5) form. The method requires a visual estimation of the local time when the surface water dries from a canopy. The presented procedure, however, has the potential to greatly improve water balance scheduling and the adoption of the ET-based scheduling method in microclimates where fog, dew, and light rainfall are common.

## References

- Allen RG, Walter IA, Elliott RL, Howell TA, Itenfisu D, Jensen ME, Snyder RL (2005) The ASCE standardized reference evapotranspiration equation. American Society of Civil Engineers, Reston, p 59
- Dawson TE (1998) Fog in California redwoods forest: ecosystem inputs and use by plant. *Oecologia* 117:476–485
- Doorenbos J, Pruitt WO (1977) Crop water requirements. FAO Irrigation and Drainage Paper 24. FAO of the United Nations, Rome, p 144
- Jacobs AFG, Heusinkveld BG, Wichink Kruit RJ, Berkowicz SM (2006) Contribution of dew to the water budget of a grassland area in the Netherlands. *Water Resources Res* 42:W03415. doi: [10.1029/2005WR004055](https://doi.org/10.1029/2005WR004055)
- Kataka G, Haruyasu N, Mizuo K, Hiromasa U, Yu H (2010) Numerical study of fog deposition on vegetation for atmosphere–land interactions in semi-arid and arid regions. *Agric For Meteorol* 150:340–353
- Kidron GJ (1999) Altitude dependent dew and fog in the Negev Desert, Israel. *Agric For Meteorol* 96:1–8
- Letej J, Cardon GE, Kan I (2007) Irrigations and uniformity. In: Lascano RJ, Viney MK, Hatfield JL, Baker JM (eds) *Irrigation of agricultural crops*. Agron Ser No. 30 American Society of Agronomy, Crop Science of America, Soil Science Society of America, Madison, WI, pp 119–131
- Mildenberger K, Beiderwieden E, Hsia YJ, Klemm O (2009)  $CO_2$  and water vapor fluxes above a subtropical mountain cloud forest—the effect of light conditions fog. *Agric For Meteorol* 149:1730–1736
- Moro MJ, Were A, Villagarcía L, Cantón Y, Domingo F (2007) Dew measurement by eddy covariance and wetness sensor in a semiarid ecosystem of SE Spain. *J Hydrol* 335:295–302
- Prada S, de Sequira MM, Figueira C, da Silva MO (2009) Fog precipitation and rainfall interception in the natural forest of Madeira. *Agric For Meteorol* 149:1179–1187
- Sentelhas PC, Gillespie TJ, Gleason ML, Monteiro JEBM, Pezzopane JRM, Pedro MJ Jr (2006) Evaluation of a Penman–Monteith approach to provide ‘reference’ and crop canopy leaf wetness duration estimates. *Agric For Meteorol* 141:105–117
- Snyder RL, Pruitt WO (1992) Evapotranspiration data management in California. In: *Proceedings water forum '92—Irrigation & drain session*. ASCE, New York